![TU Delft logo]

Delft University of Technology

A Single-sided Representation for Virtual Sources and Virtual Receivers

Wapenaar, Kees; Thorbecke, Jan Willem; van der Neut, Joost; Singh, S; Slob, Evert; Snieder, R

Citation (APA)
Wapenaar, K., Thorbecke, J. W., van der Neut, J., Singh, S., Slob, E., & Snieder, R. (2016). A Single-sided Representation for Virtual Sources and Virtual Receivers. In *78th EAGE Conference and Exhibition 2016, Vienna, Austria* (pp. 1-5). EAGE. https://doi.org/10.3997/2214-4609.201600623

Important note
To cite this publication, please use the final published version (if applicable).
Please check the document version above.

A Single-sided Representation for Virtual Sources and Virtual Receivers

K. Wapenaar* (Delft University of Technology), J.W. Thorbecke (Delft University of Technology), J.R. van der Neut (Delft University of Technology), S. Singh (Colorado School of Mines), E.C. Slob (Delft University of Technology) & R. Snieder (Colorado School of Mines)

SUMMARY

Virtual sources can be created in several ways. In seismic interferometry, a virtual source is created by crosscorrelating responses at different receivers, which are illuminated from all directions. Seismic interferometry can be mathematically described by the homogeneous Green's function representation, which is a closed boundary integral.

Virtual sources can also be created with the Marchenko method. For the Marchenko method it is sufficient that the position of the virtual source is illuminated from one side. We derive a single-sided homogeneous Green's function representation, which is an open boundary integral along reflection measurements at the surface. Applying this representation, we obtain virtual sources and virtual receivers in the subsurface from real sources and receivers at the surface (note that in our earlier work on the Marchenko method the response to the virtual source was only obtained for receivers at the surface). The retrieved virtual data show the entire evolution of the response to a virtual source in the subsurface, including primary and multiple scattering at unknown interfaces.

Introduction

Virtual seismic sources can be created in several ways. In seismic interferometry, a virtual source is created by crosscorrelating responses at different receivers. An underlying assumption is that the receiver which will be turned into a virtual source is illuminated from all directions. This is for example the case when the primary sources are distributed along a closed boundary. This situation is mathematically described by the homogeneous Green's function representation (Porter, 1970; Oristaglio, 1989). With this representation, the homogeneous Green's function $G_{\mathrm{h}}(\mathbf{x}_A, \mathbf{x}_B, t) = G(\mathbf{x}_A, \mathbf{x}_B, t) + G(\mathbf{x}_A, \mathbf{x}_B, -t)$ is expressed in terms of a closed boundary integral.

More recently it has been shown that virtual sources can be created with the Marchenko method (Broggini and Snieder, 2012; Broggini et al., 2014; Wapenaar et al., 2014; van der Neut et al., 2015). Unlike seismic interferometry, the Marchenko method does not require an actual receiver at the position of the virtual source and, equally important, the position of the virtual source needs only be illuminated from one side. Using reflection experiments at the Earth's surface and an estimate of the direct waves between the virtual source and the surface, it is possible to create the response to the virtual source, observed by receivers at the surface. Recently we have shown that it is also possible to obtain the response to the virtual source, observed by virtual receivers in the subsurface, again from reflection measurements at the surface (Wapenaar et al., 2016). Mathematically this is described by a single-sided homogeneous Green's function representation. With this representation the homogeneous Green's function $G_{\mathrm{h}}(\mathbf{x}_A, \mathbf{x}_B, t) = G(\mathbf{x}_A, \mathbf{x}_B, t) + G(\mathbf{x}_A, \mathbf{x}_B, -t)$ is expressed in terms of an open boundary integral. Originally we derived this representation by showing how a part of the closed boundary integral in the classical homogeneous Green's function representation vanishes if we introduce a specific auxiliary function in this representation. Here we present an alternative derivation of the single-sided homogeneous Green's function representation and illustrate it with a numerical example.

The classical homogeneous Green's function representation

We start with Rayleigh's reciprocity theorem (Fokkema and van den Berg, 1993) for two acoustic states A and B in a domain $\mathbb{D}$ enclosed by boundary $\partial\mathbb{D}$ with outward pointing normal $\mathbf{n} = (n_1, n_2, n_3)$. In the frequency domain this theorem reads

$$\int_{\mathbb{D}} \{q_A p_B - p_A q_B\} \mathrm{d}^3\mathbf{x} = \oint_{\partial\mathbb{D}} \frac{1}{j\omega\rho} \{p_A \partial_i p_B - (\partial_i p_A) p_B\} n_i \mathrm{d}^2\mathbf{x}. \tag{1}$$

Here q_A and p_A are the source (volume injection-rate density) and wave field (acoustic pressure) in state A, whereas q_B and p_B are these quantities in state B. Furthermore, ρ is the mass density, ω denotes angular frequency, j is the imaginary unit and ∂_i denotes differentiation with respect to x_i. Einstein's summation convention applies to repeated subscripts. The medium parameters for states A and B are identical in $\mathbb{D}$, hence, the two states obey the same wave equation in $\mathbb{D}$, but at and outside $\partial\mathbb{D}$ the medium parameters may be different. Because of the time-reversal invariance of the wave equation, the complex conjugates $-q_A^*$ and p_A^* obey the same wave equation as q_A and p_A. Making these replacements in equation (1) we obtain a second form of Rayleigh's reciprocity theorem (Bojarski, 1983)

$$\int_{\mathbb{D}} \{q_A^* p_B + p_A^* q_B\} \mathrm{d}^3\mathbf{x} = \oint_{\partial\mathbb{D}} \frac{-1}{j\omega\rho} \{p_A^* \partial_i p_B - (\partial_i p_A^*) p_B\} n_i \mathrm{d}^2\mathbf{x}. \tag{2}$$

Substituting $q_A = \delta(\mathbf{x} - \mathbf{x}_A)$, $p_A = G(\mathbf{x}, \mathbf{x}_A, \omega)$, $q_B = \delta(\mathbf{x} - \mathbf{x}_B)$ and $p_B = G(\mathbf{x}, \mathbf{x}_B, \omega)$ into equation (2), with $\mathbf{x}_A$ and $\mathbf{x}_B$ both situated in $\mathbb{D}$, gives (Porter, 1970; Oristaglio, 1989; Wapenaar and Fokkema, 2006)

$$G_{\mathrm{h}}(\mathbf{x}_A, \mathbf{x}_B, \omega) = \oint_{\partial\mathbb{D}} \frac{-1}{j\omega\rho(\mathbf{x})} \{G^*(\mathbf{x}, \mathbf{x}_A, \omega)\partial_i G(\mathbf{x}, \mathbf{x}_B, \omega) - \partial_i G^*(\mathbf{x}, \mathbf{x}_A, \omega)G(\mathbf{x}, \mathbf{x}_B, \omega)\} n_i \mathrm{d}^2\mathbf{x}, \tag{3}$$

see Figure 1(a). Here $G_{\mathrm{h}}(\mathbf{x}_A, \mathbf{x}_B, \omega) = G(\mathbf{x}_A, \mathbf{x}_B, \omega) + G^*(\mathbf{x}_A, \mathbf{x}_B, \omega) = 2\Re\{G(\mathbf{x}_A, \mathbf{x}_B, \omega)\}$ (with $\Re$ denoting the real part) stands for the homogeneous Green's function (i.e., a solution of the wave equation without a source term on the right-hand side). Equation (3) is exact, but its practical use is limited because measurements are usually not available on a closed boundary. In the next section we derive a single-sided representation for $G_{\mathrm{h}}(\mathbf{x}_A, \mathbf{x}_B, \omega)$, which can be applied in practice when measurements are available on an open boundary, see Figure 1(b).
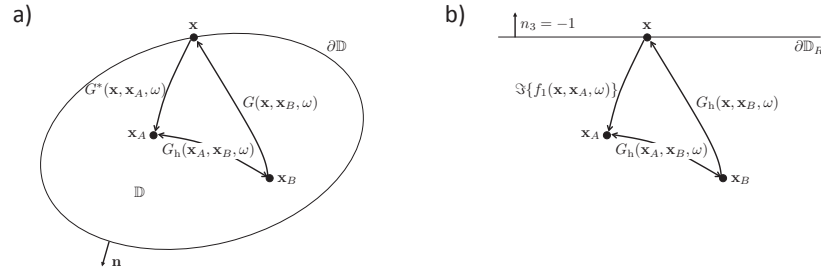
Figure 1 *(a) Visualisation of the classical homogeneous Green's function representation (equation 3). (b) Visualisation of the single-sided homogeneous Green's function representation (equation 10). Both representations account for primaries and multiples.*

Single-sided homogeneous Green's function representation

We redefine $\mathbb{D}$ as the domain enclosed by two horizontal boundaries $\partial\mathbb{D}_R$ and $\partial\mathbb{D}_A$, and a cylindrical boundary $\partial\mathbb{D}_{\text{cyl}}$. Here $\partial\mathbb{D}_R$ is the accessible boundary of the medium where the measurements take place. For simplicity we will assume it is a horizontal boundary, defined by $x_3 = x_{3,R}$. Furthermore, $\partial\mathbb{D}_A$ is a horizontal boundary at the depth of $\mathbf{x}_A$, hence, it is defined by $x_3 = x_{3,A}$. Finally, $\partial\mathbb{D}_{\text{cyl}}$ is a cylindrical boundary with a vertical axis through $\mathbf{x}_A$ and infinite radius. This cylindrical boundary exists between $\partial\mathbb{D}_R$ and $\partial\mathbb{D}_A$ and closes the boundary $\partial\mathbb{D}$. The contribution of the boundary integral over $\partial\mathbb{D}_{\text{cyl}}$ in equations (1) and (2) vanishes (but in equation (2) for another reason than Sommerfeld's radiation condition (Wapenaar et al., 1989)). We modify equations (1) and (2) for this new configuration by replacing $\partial\mathbb{D}$ by $\partial\mathbb{D}_R \cup \partial\mathbb{D}_A$, using $\mathbf{n} = (0,0,-1)$ on $\partial\mathbb{D}_R$ and $\mathbf{n} = (0,0,+1)$ on $\partial\mathbb{D}_A$. Moreover, on $\partial\mathbb{D}_A$ we apply decomposition into downgoing ($+$) and upgoing ($-$) waves (Wapenaar et al., 1989). Hence

$$\int_{\mathbb{D}} \{q_A p_B - p_A q_B\} \mathrm{d}^3\mathbf{x} = -\int_{\partial\mathbb{D}_R} \frac{1}{j\omega\rho} \{p_A \partial_3 p_B - (\partial_3 p_A) p_B\} \mathrm{d}^2\mathbf{x} - \int_{\partial\mathbb{D}_A} \frac{2}{j\omega\rho} \{(\partial_3 p_A^+) p_B^- + (\partial_3 p_A^-) p_B^+\} \mathrm{d}^2\mathbf{x},$$

(4)

$$\int_{\mathbb{D}} \{q_A^* p_B + p_A^* q_B\} \mathrm{d}^3\mathbf{x} = \int_{\partial\mathbb{D}_R} \frac{1}{j\omega\rho} \{p_A^* \partial_3 p_B - (\partial_3 p_A^*) p_B\} \mathrm{d}^2\mathbf{x} + \int_{\partial\mathbb{D}_A} \frac{2}{j\omega\rho} \{(\partial_3 p_A^+)^* p_B^+ + (\partial_3 p_A^-)^* p_B^-\} \mathrm{d}^2\mathbf{x}.$$

(5)

The downgoing and upgoing fields are pressure-normalised, hence, $p_A^+ + p_A^- = p_A$ and $p_B^+ + p_B^- = p_B$. Equation (4) is exact, whereas in equation (5) evanescent wave components on $\partial\mathbb{D}_A$ are neglected. We use equations (4) and (5) to derive a single-sided representation for the homogeneous Green's function. To this end we introduce a focusing function $f_1(\mathbf{x}, \mathbf{x}_A, \omega)$, where $\mathbf{x}_A$ denotes the focal point on $\partial\mathbb{D}_A$. We define the focusing function in a reference medium, which is identical to the actual medium in $\mathbb{D}$, but homogeneous above $\partial\mathbb{D}_R$ and below $\partial\mathbb{D}_A$. We explicitly write the focusing function as a superposition of its downgoing and upgoing constituents, according to

$$f_1(\mathbf{x}, \mathbf{x}_A, \omega) = f_1^+(\mathbf{x}, \mathbf{x}_A, \omega) + f_1^-(\mathbf{x}, \mathbf{x}_A, \omega),$$
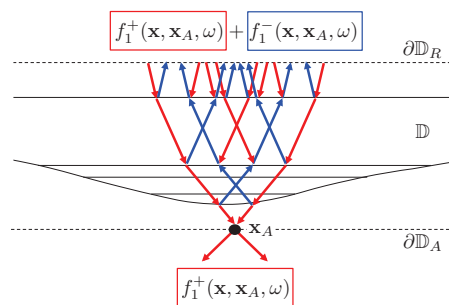
(6)

Figure 2 *Focusing function $f_1(\mathbf{x}, \mathbf{x}_A, \omega) = f_1^+(\mathbf{x}, \mathbf{x}_A, \omega) + f_1^-(\mathbf{x}, \mathbf{x}_A, \omega)$ in the reference medium.*

see Figure 2. The downgoing field $f_1^+(\mathbf{x},\mathbf{x}_A,\omega)$ is incident to the reference medium from the homogeneous upper half-space ($x_3 < x_{3,R}$). This field is shaped such that at the focal depth $x_3 = x_{3,A}$ the following conditions are obeyed (Wapenaar et al., 2014; Slob et al., 2014)

$$\partial_3 f_1^+(\mathbf{x},\mathbf{x}_A,\omega)|_{x_3=x_{3,A}} = -\tfrac{1}{2} j\omega\rho(\mathbf{x})\delta(\mathbf{x}_H - \mathbf{x}_{H,A}), \tag{7}$$

$$\partial_3 f_1^-(\mathbf{x},\mathbf{x}_A,\omega)|_{x_3=x_{3,A}} = 0. \tag{8}$$

Here $\mathbf{x}_H$ stands for the horizontal components of the coordinate vector, hence, $\mathbf{x}_H = (x_1,x_2)$ and $\mathbf{x}_{H,A} = (x_{1,A},x_{2,A})$. The factor $-\tfrac{1}{2} j\omega\rho(\mathbf{x})$ is chosen for convenience. At and below the focal depth there is no up-going field because the reference medium is homogeneous below this depth. A focusing function which exactly obeys condition (7) is unstable in the evanescent field. In the following we exclude evanescent wave components and tacitly assume that the spatial delta function in equation (7) is band limited. The focusing function $f_1(\mathbf{x},\mathbf{x}_A,\omega)$, defined in the reference medium, will play the role of state A in equations (4) and (5). The Green's function $G(\mathbf{x},\mathbf{x}_B,\omega)$, defined in the actual medium, will play the role of state B. Its source at $\mathbf{x}_B$ may lie above or below $\mathbf{x}_A$. Substituting $p_A^\pm(\mathbf{x},\omega) = f_1^\pm(\mathbf{x},\mathbf{x}_A,\omega)$, $q_A(\mathbf{x},\omega) = 0$, $p_B^\pm(\mathbf{x},\omega) = G^\pm(\mathbf{x},\mathbf{x}_B,\omega)$ and $q_B(\mathbf{x},\omega) = \delta(\mathbf{x} - \mathbf{x}_B)$ into equations (4) and (5), using equations (6) − (8) and $G(\mathbf{x},\mathbf{x}_B,\omega) = G^+(\mathbf{x},\mathbf{x}_B,\omega) + G^-(\mathbf{x},\mathbf{x}_B,\omega)$, and summing the results, gives

$$G(\mathbf{x}_A,\mathbf{x}_B,\omega) + H(x_{3,A} - x_{3,B}) 2j\Im\{f_1(\mathbf{x}_B,\mathbf{x}_A,\omega)\} \tag{9}$$

$$= \int_{\partial\mathbb{D}_R} \frac{2}{\omega\rho(\mathbf{x})} \Big(\Im\{f_1(\mathbf{x},\mathbf{x}_A,\omega)\}\partial_3 G(\mathbf{x},\mathbf{x}_B,\omega) - \Im\{\partial_3 f_1(\mathbf{x},\mathbf{x}_A,\omega)\}G(\mathbf{x},\mathbf{x}_B,\omega) \Big) \mathrm{d}^2\mathbf{x},$$

where $H(x_3)$ is the Heaviside function and $\Im$ denotes the imaginary part. Taking the real part of both sides of this equation gives

$$G_h(\mathbf{x}_A,\mathbf{x}_B,\omega) = \int_{\partial\mathbb{D}_R} \frac{2}{\omega\rho(\mathbf{x})} \Big(\Im\{f_1(\mathbf{x},\mathbf{x}_A,\omega)\}\partial_3 G_h(\mathbf{x},\mathbf{x}_B,\omega) - \Im\{\partial_3 f_1(\mathbf{x},\mathbf{x}_A,\omega)\}G_h(\mathbf{x},\mathbf{x}_B,\omega) \Big) \mathrm{d}^2\mathbf{x}. \tag{10}$$

This is the single-sided representation of the homogeneous Green's function, see Figure 1(b). The Green's function $G(\mathbf{x},\mathbf{x}_B,\omega)$ in the right-hand side can be expressed in a similar way, according to

$$G_h(\mathbf{x},\mathbf{x}_B,\omega) = \int_{\partial\mathbb{D}_S} \frac{2}{\omega\rho(\mathbf{x}')} \Big(\Im\{f_1(\mathbf{x}',\mathbf{x}_B,\omega)\}\partial_3' G_h(\mathbf{x},\mathbf{x}',\omega) - \Im\{\partial_3' f_1(\mathbf{x}',\mathbf{x}_B,\omega)\}G_h(\mathbf{x},\mathbf{x}',\omega) \Big) \mathrm{d}^2\mathbf{x}', \tag{11}$$

with $\mathbf{x}$ on $\partial\mathbb{D}_R$ and $\mathbf{x}'$ on $\partial\mathbb{D}_S$, just above $\partial\mathbb{D}_R$. Note that $G(\mathbf{x},\mathbf{x}',\omega)$ stands for the reflection response at the surface. Hence, equations (10) and (11) together describe redatuming of $G(\mathbf{x},\mathbf{x}',\omega)$ from the surface, yielding $G_h(\mathbf{x}_A,\mathbf{x}_B,\omega)$ in the subsurface. The required focusing functions can be derived from the reflection response at the surface and an estimate of the direct arrivals, using the iterative Marchenko method (Wapenaar et al., 2014). The entire redatuming process is illustrated in Figure 3. Figure 3(a) shows a 2D inhomogeneous medium. We modelled the reflection responses $G(\mathbf{x},\mathbf{x}',\omega)$ for 600 sources and 600 receivers, with a horizontal spacing of 10 m, at the upper boundary. The central frequency of the band-limited source function is 30 Hz. We use the Marchenko method to obtain the focusing functions and substitute these into equation (11) to redatum the sources from $\mathbf{x}'$ to $\mathbf{x}_B$, and subsequently into equation (10) to redatum the receivers from $\mathbf{x}$ to $\mathbf{x}_A$. We thus obtain $G_h(\mathbf{x}_A,\mathbf{x}_B,\omega)$, or in the time domain $G_h(\mathbf{x}_A,\mathbf{x}_B,t) = G(\mathbf{x}_A,\mathbf{x}_B,t) + G(\mathbf{x}_A,\mathbf{x}_B,-t)$. Figures 3(b), (c) and (d) show snapshots of this function for $t = 0.004$ s, $t = 0.15$ s and $t = 0.30$ s, respectively, each time for fixed $\mathbf{x}_B = (0,800)$ and variable $\mathbf{x}_A$.

Conclusions

We have presented a straightforward derivation of single-sided homogeneous Green's function representations, which can be used to create virtual sources and virtual receivers in the subsurface from the reflection response at the surface and an estimate of the direct arrivals. An illustration of the application of these representations is given in Figure 3. Note that no information about the positions and shapes of the scattering interfaces has been used, yet this virtual response clearly shows how scattering occurs at the interfaces. A multiple-free image can be obtained by selecting $G_h(\mathbf{x}_B,\mathbf{x}_B,t=0)$ for all $\mathbf{x}_B$ of interest. However, $G_h(\mathbf{x}_A,\mathbf{x}_B,t)$ contains a wealth of additional information (including local AVA), of which the applications will be further investigated. One of the many potential applications is the prediction of the propagation of micro-seismic signals through an unknown earth.
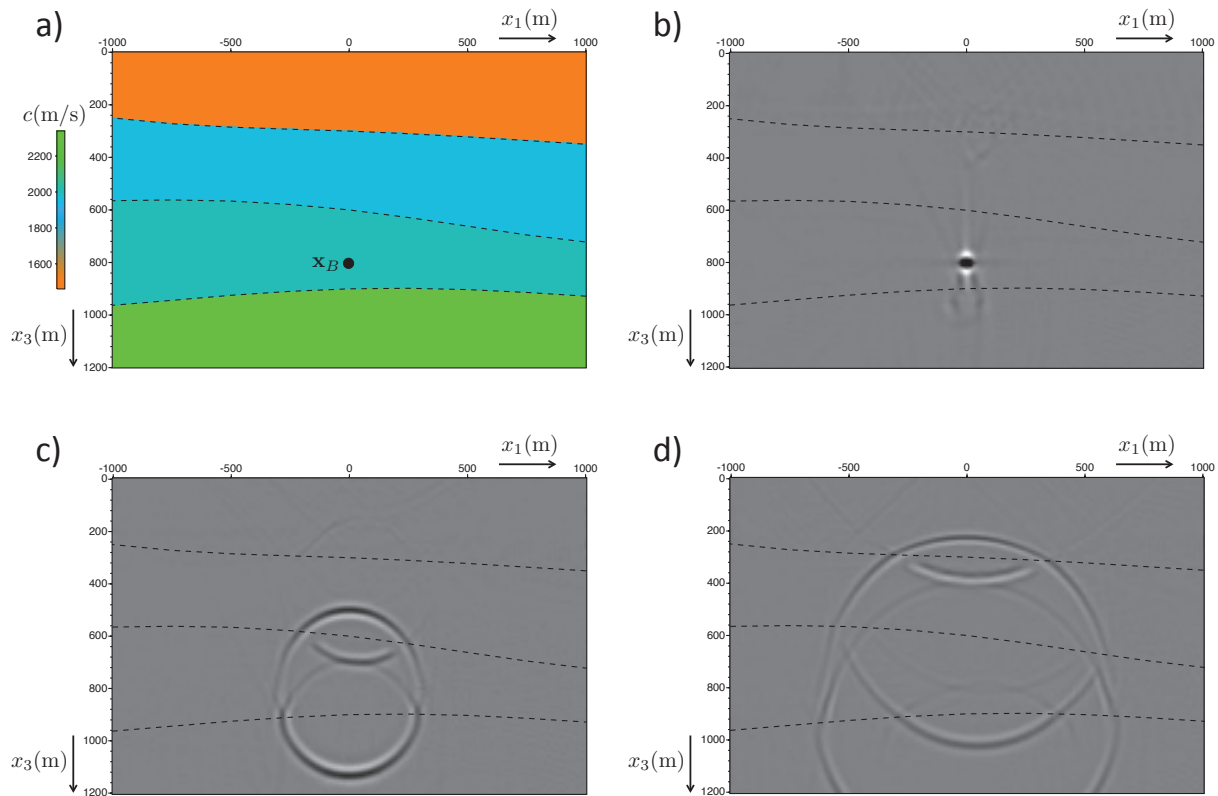
Figure 3 *Numerical example, illustrating the application of the single-sided homogeneous Green's function representations (equations 10 and (11)). (a) Inhomogeneous medium. (b) Snapshot of $G(\mathbf{x}_A, \mathbf{x}_B, t) + G(\mathbf{x}_A, \mathbf{x}_B, -t)$ at $t = 0.004$ s, for fixed $\mathbf{x}_B = (0, 800)$ and variable $\mathbf{x}_A$. (c) Idem, for $t = 0.15$ s. (d) Idem, for $t = 0.30$ s.*

References

Bojarski, N.N. [1983] Generalized reaction principles and reciprocity theorems for the wave equations, and the relationship between the time-advanced and time-retarded fields. *Journal of the Acoustical Society of America*, **74**, 281–285.

Broggini, F. and Snieder, R. [2012] Connection of scattering principles: a visual and mathematical tour. *European Journal of Physics*, **33**, 593–613.

Broggini, F., Snieder, R. and Wapenaar, K. [2014] Data-driven wavefield focusing and imaging with multidimensional deconvolution: Numerical examples for reflection data with internal multiples. *Geophysics*, **79**(3), WA107–WA115.

Fokkema, J.T. and van den Berg, P.M. [1993] *Seismic applications of acoustic reciprocity*. Elsevier, Amsterdam.

van der Neut, J., Wapenaar, K., Thorbecke, J., Slob, E. and Vasconcelos, I. [2015] An illustration of adaptive Marchenko imaging. *The Leading Edge*, **34**, 818–822.

Oristaglio, M.L. [1989] An inverse scattering formula that uses all the data. *Inverse Problems*, **5**, 1097–1105.

Porter, R.P. [1970] Diffraction-limited, scalar image formation with holograms of arbitrary shape. *Journal of the Optical Society of America*, **60**, 1051–1059.

Slob, E., Wapenaar, K., Broggini, F. and Snieder, R. [2014] Seismic reflector imaging using internal multiples with Marchenko-type equations. *Geophysics*, **79**(2), S63–S76.

Wapenaar, C.P.A., Peels, G.L., Budejicky, V. and Berkhout, A.J. [1989] Inverse extrapolation of primary seismic waves. *Geophysics*, **54**(7), 853–863.

Wapenaar, K. and Fokkema, J. [2006] Green's function representations for seismic interferometry. *Geophysics*, **71**(4), SI33–SI46.

Wapenaar, K., Thorbecke, J. and van der Neut, J. [2016] A single-sided homogeneous Green's function representation for holographic imaging, inverse scattering, time-reversal acoustics and interferometric Green's function retrieval. *Geophysical Journal International*, **204**, in press.

Wapenaar, K., Thorbecke, J., van der Neut, J., Broggini, F., Slob, E. and Snieder, R. [2014] Marchenko imaging. *Geophysics*, **79**(3), WA39–WA57.